TWO-DIMENSIONAL WIND TUNNEL TESTS ON A CONVENTIONAL WING SECTION OVER A WIDE RANGE OF REYNOLDS NUMBERS AND UP TO HIGH SUBSONIC FREE-STREAM SPEEDS

D. Brown
National Research Council of Canada
Ottawa, Canada

ABSTRACT

Pressure distributions, overall forces and local shear stresses were obtained in the wind tunnel at Mach and Reynolds numbers which are achieved in full-scale flight with large aircraft for the NACA65_1-213(a=0.5) section.

The very high Reynolds number capability has been achieved through the use of a relatively narrow test duct and wall boundary-layer removal is necessary to approximate to two-dimensional flow. The strong normal shock associated with this 'conventional' wing section is usually found to be curved in its intersection with the wing surface and the curvature is strongly affected by the amount of sidewall boundary layer removal. A further problem noted is that of a non-uniform wake drag in the spanwise sense. The degree of non uniformity is Reynolds number dependent.

Upper surface shock wave position is found to vary little over a wide Reynolds number range if the shock occurs for a certain combination of Mach number and normal force e.g. M = .76, C_n = 0.1 but the movement may be considerably increased with higher values.

1. INTRODUCTION

Owing to the nature of wind tunnel testing - in limited cross section streams which inevitably suffer to some degree from wall boundary layer growth, and usually have a turbulence level and scale different from that of the atmosphere - results of model tests have to be treated with some reserve. The reservations grow when we conduct tests at subsonic "free-stream" Mach numbers high enough to generate strong normal shock waves on the model. The attendant interactions between the normal shock waves and the wall boundary layers,especially in the case of "two-dimensional" tests on wings completely spanning the test duct,can give rise to considerable doubt about the validity of the tests. For this reason at least, comparisons with flight measurement are valuable but none too easy to come by on a casual basis.

For a number of years there has been a realisation of the significance of shock wave/boundary-layer interaction and of the consequence of extrapolation of low Reynolds number wind tunnel data (1.5 - 3.0x10^6 on wing chord) to assist the design of large aircraft[8].

As a result,there is now considerable effort being expended in acquiring large new transonic test facilities capable of testing complete aircraft models at Reynolds numbers overlapping typical full-scale values. In the interim a number of existing wind tunnels have incorporated modifications to carry out two-dimensional aerofoil tests at about flight values of Reynolds number. One of the earliest examples of these has been the NAE 5 ft x 5 ft blowdown wind tunnel. This facility was provided with a"two-dimensional flow" insert for the normal transonic working section. The design point for the modified facility was set as a unit Reynolds number of 40x10^6 per foot at M = 1. To achieve this and a steady run time in the neighbourhood of 10 seconds required a working-section width of fifteen inches in conjunction with the normal working-section height of 60 inches. The lowest practicable chord for aerofoils is in the neighbourhood of 10 inches, bending strength of partly hollow pressure recording models being a limitation. As a result of the relatively low aspect ratio it is vital to remove a large fraction of the sidewall boundary layer to obtain acceptably two-dimensional flow. This procedure has led to shock-wave curvature problems in some cases.

As in other facilities[5],the measurement of wake-drag has led to finding spanwise non-uniformities. The causes of these are still unresolved although some progress has been made in unmasking the underlying reasons.

The measurement of detailed surface pressure distributions on the NACA 65_1-213, (a=0.5) section,over a range of chord Reynolds numbers which overlap flight values on moderately large aircraft(12-53x 10^6), at Mach numbers which produce strong upper surface normal shocks,has afforded some information on shock wave locations not previously obtained.

Our confidence in these results, in view of the findings regarding shock curvature rests more in the general trend of shock wave movement than in its actual position at any particular combination of Mach number,Reynolds number and normal force.

The findings in this paper relate to the NACA 65_1-213 (a=0.5) aerofoil section but some of the conclusions are more or

less applicable to any section that incurs a strong upper surface shock-wave. In particular strongly curved shocks have also been observed on an NACA 0012 section model tested in the NAE "two-dimensional" insert, and to a lesser extent, on a slightly modified NACA 65_2-215 section model.

The measurement of skin friction, on aerofoil surfaces, for high Reynolds numbers has not been very frequently reported. Among the most active in this endeavour have been a research group at R.A.E. who have derived valuable data during extensive and significant tests on aerofoils in low speed and at high subsonic Mach numbers for chord Reynolds numbers up to 15×10^6. They have promoted the use of razor blades (Stanton tubes) as devices for the indirect measurement of skin friction on aerofoils and we have used their form of a calibration equation relating surface shear stress to the pitot pressure recorded at the device[10].

Upper and lower surface shear stress coefficients have been obtained on the NACA 65_1-213(a=.5) aerofoil for a nominal freestream Mach number of 0.7 at chord Reynolds numbers up to 25×10^6 and normal force coefficients from zero to 0.5 approximately.

2. TEST FACILITY, MODEL AND FLIGHT TEST AIRCRAFT

2.1 Facility

The two-dimensional insert associated with the NAE 5 ft x 5 ft blowdown wind tunnel has been described in some detail elsewhere[1] [2] [3] and only the briefest description is now necessary.

Through the use of the insert, it is possible to conduct "two-dimensional" tests on aerofoil sections and obtain unit Reynolds numbers of between 9.6 and 42.5×10^6 per foot for "freestream" Mach numbers in the range of 0.7 to 0.8. The lower limit to Reynolds number is determined by the ability to remove sufficient wall boundary layer to set up acceptably two-dimensional flow, while the upper limit is determined by the compressed air supply.

The duct is 15 inches wide with solid sidewalls and 20.5% open, perforated floor and ceiling. It has been customary to test 10" or 15" chord wings which effectively span the duct. The small clearance between the wing tip and the wall, which allows attitude changes, is sealed with lightly sprung teflon sealing strips. Strain gauge balances, built into the sidewalls at mid-height, support the model and enable the measurement of normal and chordwise forces and aerofoil pitching moments. Sidewall boundary layers in the vicinity of the model are more or less removed through a porous section of each sidewall (18 inches wide x 24 inches streamwise) which surrounds the aerofoil contour. This is obtained by allowing a small amount of the flow (about 0.5% of the tunnel mass flow) to vent to atmosphere through adjustable valves.

Aerofoil pressure measurements can be obtained by use of fast scanning pressure switches and wake pressure measurements are made if required at a fixed location downstream of the balances' centre. For a 15 inch chord model this places the traverse plane approximately 0.8 chord lengths behind the trailing-edge, as shown in Fig.2(a). It is normal practice to use a four pitot-tube wake-rake which is traversed in the vertical direction to maximum excursions of 20 inches and 10 inches above and below the tunnel centre-line at speeds of up to 10 inches per second. The traversing speed can be arranged to be an inverse function of wake total pressure gradients - automatically slowing down in regions of high shear and moving quickly through areas of uniform pressure.

2.2 The Model

The results to be subsequently discussed were obtained following tests on a 15 inch chord model of NACA 65_1-213(a=0.5) aerofoil section (Fig.2(a)). The model was constructed in stainless steel to a high degree of accuracy and polished to a 4 micro-inch finish. Forty-nine pressure orifices were installed in the upper and lower surfaces (thirty-one in the upper surface, one each at leading and trailing-edges and the remainder in the lower surface along the centre line). A subsidiary line of eighteen orifices was provided in the upper surface, 4 inches off the centre line (2 y/b=0.53) and three orifices were placed in the lower surface at the same offset from the centre-line. With the exception of the trailing-edge orifice which was a rectangular slit, (0.004"x0.25") the others were circular and 0.013 inches in diameter.

The orifices' spacing was mainly uniform with an interval of 0.05 in x/c except for $0.525 \leq x/c \leq 0.6$, where the spacing was decreased by a factor of four, to more accurately sense the position of the upper surface shock wave by pressure measurement.

For the indirect measurement of upper and lower surface skin friction, Stanton tubes were used. These were made by using small pieces of commercial razor blade (0.1"x0.1" and 0.004" thick) in conjunction with surface orifices to form a surface pitot tube.

2.3 Flight Test Aircraft

A limited amount of comparison between the results of flight measurements of

surface pressure distribution and pressures measured in the NAE two-dimensional insert is possible. The flight measurements were reported in 1947[4] and they reflect the state of the art at that time - for instance wing pressures were measured using liquid manometers housed in the fuselage nose compartment of the Lockheed F80-A aircraft. The claims for accuracy of measurements of various quantities associated with the flight tests are as follows:

Mach number ± .005
Pressure altitude ±50 ft
Measured pressure coefficient 10/q
(where q is the dynamic pressure in lb/ft^2)

Pressure distributions on the aircraft were measured at four spanwise locations as shown in Fig.2(b). For comparison purposes, only the results from the 105 inch and the 152 inch stations on the aircraft are considered. The inboard and outboard stations are considered to be so close to the fuselage and wing tip respectively, that local effects would impose themselves on the section characteristics. The leading edge sweepback of 9° is considered to be too low to have a noticeable effect on the section characteristics at stations 105" and 152". Although the instrumented section at station 152" did intersect the aileron, the piano type hinge would effectively seal the gap.

As may be expected the section profile on the aircraft was less accurate than that of the wind tunnel model due to construction using thin sheet metal rivetted to relatively solid wing spars. As a result, there is some waviness on the upper surface, over the front and rear 30%, as shown in Fig.3 but it is felt that the profile closely follows the design geometry.* The accuracy of the profile at station 152" on the aircraft was equally as good as that of station 105". It is thought unlikely that air loads would produce significant changes in the profiles on the aircraft.

3. RESULTS

3.1 Pressure Distributions

Fig.4(a) shows an example of good agreement between a pressure distribution measured on the model and that measured in flight[4]. The comparison is a significant one, in that the free-stream Mach number of 0.75 and the angle of attack are both large enough to cause a strong shock-wave on the upper surface. It is unfortunate that the test conditions do not coincide more exactly in Reynolds number but it is probably fair to say that the test conditions set up in the wind tunnel are an adequate representation of the flow over the aircraft wing at a section chosen for its remoteness both from the flow as affected by the fuselage and by the wing tip. It will be observed that, with respect to normal force, pitching moment, shock wave position and post shock-wave pressure, agreement is good. For this Mach number it appears that the simple method of removing the wall boundary layer in the vicinity of the model by allowing approximately 0.5% of the mass flow to bleed away to atmosphere, without any attempt to distribute the normal flow in any particular way, sets up proper flow conditions.

Figs.4(b) and 4(c) demonstrate that considerably less satisfactory results are obtained at a higher Mach number. The Mach numbers, both in the wind tunnel test and flight are close, as are the Reynolds numbers but the matching of C_n is poorer than formerly. In Fig.4(b) the major discrepancy is that the post shock-wave pressure recovery is considerably less in the wind-tunnel test than in the flight case. This suggests that if a falling pressure at some point on the upper surface near the trailing edge (e.g. at 95% chord) was used as a buffet onset indicator the wind tunnel test result would give a conservative result. In Fig.4(c) wind-tunnel test results are compared with flight measurements for a much higher loading case. The free-stream conditions are very close in this case and the values of C_n agree within 5%. There is complete separation behind the normal-shock in each case with good pressure agreement on the upper surface. On the lower surface the flow is wholly subcritical in the wind-tunnel test, whereas a small supersonic region is indicated in the flight measurement. The major discrepancy however is that the upper surface normal-shock-wave in the flight case is considerably further forward (approximately 5% of chord) than indicated by the pressure measurements made on the model.

The results shown in Figs.4(b) and 4(c) suggest that, for this particular aerofoil section, the accuracy with which proper two-dimensional flow conditions can be set up can be seriously impaired at $M_{nom} = 0.8$. While it may be agreed that a Mach number of 0.8 lies beyond the proper range of operating conditions for this aerofoil, nevertheless, the example does point out the difficulties that can be encountered in two-dimensional tests in transonic flow, if a strong upper surface shock occurs.

Fig.5 gives wind tunnel results showing limits imposed by normal force on the validity of pressure data. In (a) the two pressure distributions shown are

---

* Fig. 3 shows that the maximum departure from the design ordinates is slightly more than 0.1 percent chord. At high speeds the waviness at front and rear might be expected to interfere more with the flow development than the increased camber of the section as a whole.

virtually co-incident. These were obtained in two separate pressure scans at a fixed angle of attack. The nominal Mach number was 0.75, the nominal Reynolds number was 45×10^6, certainly high enough to ensure thin boundary layers, and the normal force coefficient was nearly 0.5. However, an increase in the angle of attack by 1^o demonstrates a further difficulty encountered. In the second pressure scan, at the same test conditions, the upper surface normal shock wave has apparently moved forward by about 2% and C_{np} has decreased more than 1%. The time taken to scan those four pressure tappings, which register the shock-wave, was approximately 0.2 seconds. Since, in each case, the recorded pressure rise is undirectional throughout, this suggests that the shock-wave movement was quite slow.

The shock-wave movement may be a genuine aerofoil effect at high C_n but, in the absence of flight data, there remains the possibility that we have demonstrated a testing difficulty, which imposes a limit on the accuracy with which the shock position and C_n can be determined, at high subsonic Mach numbers.

The effect of boundary-layer trips on the pressure distribution was investigated by bonding carborundum grains, in narrow strips (approximately 0.25% chord), on upper and lower surfaces, at x/c = 0.05. Owing to the high shear forces it was found impossible for the grains (280 grit size) to stay attached above a Reynolds number of 17×10^6 even at $M_T = 0.7$. Fig. 6(a) to (d) gives an indication of the effect of a roughness element (240 grit size) for Re = 17×10^6 and $M_{nom} = 0.8$. The results indicate that up to moderate loading ($C_n \triangleq 0.25$), the effect of the boundary layer trip on pressure distribution is small and mainly confined to the lower surface. A local effect on the upper surface pressure distribution is noted between the leading-edge and 10% chord. However, as will be seen later, there is a strong effect on drag.

It is important that the comparisons be obtained at the same test Mach number, since, at this level, the shock-wave position critically depends on M_T. This condition was achieved in each case for the results shown in Fig. 6.

3.2 Shock Wave Position

One of the main reasons for conducting these tests over a Reynolds number range which overlaps full-scale values was to directly note the effect of Reynolds number on upper surface shock-wave position. Real shock/boundary-layer interaction interrupts the progressive downstream movement of the shock wave that would occur for inviscid flow as the free stream Mach number increases towards unity and effects temporary reversals of direction in the movement.

The position is a strong function of Mach number and normal force coefficient and Fig.7 is given to indicate the dependence of the shock position on these quantities in the range $0.7 \leq M_{nom} \leq 0.8$. The position of the shock, as defined by pressure measurement, is open to argument but in these results it is defined as shown in Fig.5(a). Having in mind the limitations that have been implied in the earlier discussion of the validity of data on shock-wave position as determined by pressure measurements in the "two-dimensional" wind tunnels, Fig.8 shows the dependence of the upper-surface shock-wave position on Reynolds number. The curves in this figure were obtained by cross-plotting the results in Fig.7 for constant values of Mach number. The upper set of results ($C_n = 0.1$) indicate a slight backwards movement of the shock wave as the Reynolds number is increased from about 12×10^6 to 53×10^6, for stream Mach numbers of 0.74 and 0.76 respectively. At some value of Mach number between 0.76 and 0.78 viscous effects start to play an increasingly important role and we see a rearward movement, at $M_T = 0.78$, of about four times as much (about 4% chord) as occurs at $M_T = 0.76$. The interaction of boundary-layer and shock-wave for $M_T = 0.78$ is such that below Re = 20×10^6 the shock is driven further forward than at $M_T = 0.76$. The higher pressure rise, which occurs for a free stream speed equivalent to $M_T = 0.8$, and the attendant strong boundary-layer interaction, causes the shock wave to be stationed ahead of the shock that occurs for $M_T = 0.76$ up to Re = 50×10^6. In that case the total shock movement over the Reynolds number range is more than 5% chord.

At $C_n = 0.3$ a similar state of affairs prevails but the effects are exaggerated, through the generally increased upper-surface boundary-layer thicknesses. At $M_T = 0.72$ and 0.74, the backward shifts in shock position are again small. For $M_T = 0.76$ there is a fairly rapid movement backwards as Re increases, from about 17×10^6 to 30×10^6, followed by a pronounced levelling off. At $M_T = 0.78$ the backward movement rate is similar but, up to the maximum value of Reynolds number, no levelling off is seen. Up to Re = 53×10^6 the shock-wave for $M_T = 0.78$ is always ahead of its counterpart at $M_T = 0.76$ and up to a Reynolds number of about 38×10^6 is even ahead of the shock wave corresponding to $M_T = 0.74$. The apparent backward shift in shock-wave position, for Reynolds numbers below about 17×10^6 ($M_T = 0.76$, 0.78 and 0.8), is believed to be due to sidewall boundary-layer growth and the inability of the simple boundary layer removal system to cope with the requirements. At $Re_{nom} = 12 \times 10^6$, the low working section pressure limited the value of V_n/U_∞ to 0.0045 or less.

3.3 Shock Wave Curvature

In the previous figure, the upper-

surface shock-wave position was taken as that defined by the pressure distribution on the centre-line. However, an interesting observation made during the investigation on this aerofoil was that of shock-wave curvature. This is illustrated in Fig.9 in which the pressure distribution sensed by the line of pressure taps offset 4 inches from the centre line taps is shown with the centre line distribution. The test condition (M_{nom} = 0.8, Re_{nom} = 45×10^6 and $\alpha_g = 1.8^o$) produce a strong shock wave which is curved in plan view to the extent of being about 2% chord (i.e. 0.3 inches) further ahead on the centre line than on the offset line. In this case the sidewall boundary layer removal velocity ratio was 0.0055, the amount that was determined during the calibration tests[1] as being sufficient to provide two-dimensional flow. The normal force coefficient C_{nb} is in this case, because of the swept back shock larger than C_{np} by 2.1%. Fig.10 shows the full extent of the curvature of the shock under various combinations of Mach number, Reynolds number and normal force.

In the M_{nom} = 0.8 cases there is complete breakdown of two-dimensional flow behind the shock wave and two cells of rotating fluid are manifest by the surface flow visualization. At M_{nom} = 0.75 and $Re_{nom} = 25 \times 10^6$ reasonably good two-dimensional flow exists behind the shock wave but, at the lower Reynolds number of 12×10^6, insufficient sidewall boundary layer removal leads to a curved forward shock-wave and strongly curved surface flow behind the shock. It is apparent from Fig.11 that the magnitude and the sense of the curvature* is strongly affected by M_T and Re and in some cases by C_n. Increasing normal force and Mach number generally promotes a rearwards curved shock wave whereas increasing Reynolds number has an opposite effect. This is especially so at the lower Mach numbers shown in Fig.11, with the exception of the results at $Re_{nom} = 25 \times 10^6$, M_T = 0.727, which run counter to this trend, over a wide range of C_{np}. The most disconcerting finding is that the highest Reynolds number flow does not appear to reduce the shock curvature, as might be expected on the grounds of the thinnest boundary-layers - indeed at the two lower Mach numbers considered the opposite effect is noted.

That the shock curvature is influenced by boundary-layer thickness is demonstrated in Fig.12. The curvature is once more plotted against C_{np} for two values of V_n/U_∞, viz 0.0054 and 0.003. The results at M_{nom} = 0.75 suggest that, at some intermediate value of V_n/U_∞, a stable and only slightly curved shock might occur. However, at the higher Mach number, the velocity ratio should vary from 0.0054 to some value less than 0.003 in the range $0 \leq C_n \leq 0.5$.

*defined as $\Delta x_s / y_\ell$

Unfortunately, varying V_n/U_∞, to minimise shock curvature, has a strong effect on the fore and aft position of the shock wave at the model centre-line. Fig.13 displays the magnitude of the changes in position for M_{nom} - 0.75 and 0.8 and a wide range of Reynolds number. Care has been taken where possible, to present results for which only C_{np} varies significantly, apart from the changes in V_n/U_∞. Although the pressure distributions of Ref.4 are difficult to interpret for snock wave location, owing to an insufficiency of pressure tappings in the upper surface, a few have been located on the curves of Fig.13, to afford a comparison between wind tunnel test and flight measurement. They demonstrate closer agreement with the curves corresponding to the higher values of V_n/U_∞.

3.4 Sidewall Boundary Layer Effect on Aerodynamic Characteristics

The effect, on the aerodynamic characteristics C_n, C_d and $C_{mc/4}$, of reducing V_n/U_∞ are shown, for M_{nom} of 0.75 and 0.8 and for Re_{nom} of 17×10^6 and 35×10^6 respectively, in Fig.14. The drag coefficients plotted (C_{dwl}), are those obtained from the wake total-pressure profile near the centre of the duct. The results at the lower Mach number (Fig.14(a)) indicate that, reducing the rate of sidewall boundary-layer removal by a factor of nearly two results in a drastic reduction in C_n, $\partial C_n/\partial\alpha$ (pressure and balance values) and also in wake-drag coefficients near the centre line. The two-dimensionality of the flow, as measured by C_n, is rather better for the V_n/U_∞ = 0.0054 case than the lower value. From our experience with other aerofoil sections and from the character of the wake drag coefficient versus angle of incidence in supercritical flow, as seen in Fig.14(a), there is no question that the higher value of V_n/U_∞ is the more appropriate.

The situation is not as clear, however, at M_{nom} = 0.8, as shown in Fig.14(b). There is now a cross-over in normal force at $C_{np} \triangleq 0.3$ and $\partial C_{np}/\partial\alpha_g$ is consistently higher for V_n/U_∞ = .003. For C_{nb}, cross-over occurs at $C_{nb} \triangleq 0.45$ but $\partial C_{nb}/\partial\alpha_g$ is consistently higher too at V_n/U_∞ = 0.003 The two-dimensionality of the flow is distinctly worse than at M_{nom} = 0.75 and there is little to choose between using V_n/U_∞ = 0.0054 and 0.003 ($|\Delta C_n|$ rises to about 4% of the maximum recorded value of C_{np}). The "centre-line" wake-drag coefficients are again considerably lower for V_n/U_∞ = 0.003 but it is found that there is far better agreement between the wake-drag coefficients and the balance measured drag-coefficients (interpolated for zero normal force) for V_n/U_∞ = 0.0054.

Thus while it appears that V_n/U_∞ = 0.0054 is the more appropriate value to use, it is clear that tests on this

particular aerofoil section in a situation demanding sidewall boundary-layer removal, at Mach numbers in excess of 0.8, could give widely misleading information.

In Figs. 15, 16 and 17 the effect of Reynolds number on the uniformity of the wake-drag coefficient at two spanwise locations, viz. 2y/b = -.13 and 0.2, is shown for M_{nom} = 0.7, 0.75 and 0.8. The drag coefficients at these stations are designated C_{dw1} and C_{dw2} respectively and comparisons are effected by plotting C_{dw1} versus C_{dw2}. It is immediately apparent that by far the greatest discrepancies between C_{dw1} and C_{dw2} occur for the lowest nominal Reynolds number i.e. 12×10^6. For M_{nom} = 0.7 (Fig.15), it should be noted that from $Re_{nom} = 12 \times 10^6$ to 25×10^6 there is a progressive improvement; above 25×10^6 however, further increases in Re do not achieve further gains - indeed at 45×10^6 it could fairly be said that the drag uniformity has reverted to the level seen at 17×10^6.

With an increase in Mach number to 0.75 (Fig.16), drag uniformity is improved over the whole range of Re and, above 12×10^6, the discrepancies are mostly considerably less than 0.1 C_{dw1}.

For M_{nom} = 0.80 (Fig.17), the discrepancies at 12×10^6 continue to diminish, while those for $Re_{nom} = 17 \times 10^6$ remain at about the same level as for M_{nom} = 0.75.

The presence of a roughness strip, at 5% chord on upper and lower surfaces, greatly improves wake drag uniformity at M = 0.7 and Reynolds numbers of 12 and 17×10^6, to a lesser extent at M_{nom} = 0.75 but achieves little for M_{nom} = 0.8. Results are given in Figs.18, 19 and 20. The improvement in uniformity is achieved at the expense of considerably increased drag, especially at M_{nom} = 0.7 and, to a lesser extent, at M_{nom} = 0.75. The drag 'buckets' at low values of C_n virtually disappear.

3.5 Aerofoil Boundary Layer

Fig.21 shows the results of attempting to visualize the aerofoil boundary-layer flow at M_{nom} = 0.7 and Reynolds numbers of 12 and 17×10^6, with natural transition. At 12×10^6, the surface flow for C_{np} = 0.12 and 0.34 is shown and for 17×10^6, C_{np} = 0.12. It appears that at $Re_{nom} = 12 \times 10^6$ laminar flow would have been maintained across the span up to s/c = 0.45, approximately, at C_{np} = 0.12 and rather less at C_{np} = 0.34 (the scale on the central photograph is 0.5 in. between major divisions) but for the turbulence wedges which occurred. At $Re_{nom} = 17 \times 10^6$ the length of laminar flow was considerably less - approximately, s/c = 0.25 - and the number of turbulent wedges was considerably more. Surface flows of this kind have been observed elsewhere with "two-dimensional" flow. The lengths of laminar flow were shorter still at $Re_{nom} = 25 \times 10^6$ and there was a proliferation of turbulence wedges. The argument could, of course, be raised that the roughness introduced by the visualization material (Titanium di-oxide suspended in kerosene) would be responsible for the wedges of turbulent flow and in its absence the lengths of laminar flow would be constant across the span. This, however, is not believed to be the case and support for non-acceptance is given in Figs.22 and 23.

Figs. 22 and 23 show profiles of shear-stress coefficient measured using the razor blade technique. Apart from a change in the numerical value of the constant Δ to 0.0004, following some high Reynolds number tests in a smooth pipe at NAE, the calibration equation used was that given in Ref. 10. In addition to the profiles on the centre-line, the friction was also measured at three chordwise stations on the offset line of tappings, at x/c = 0.4, 0.5 and 0.6

The salient feature is that at $Re_{nom} = 12 \times 10^6$ and to a lesser extent at $Re_{nom} = 17 \times 10^6$ there is poor agreement to be seen between the value of C_f on the centre line and at corresponding stations on the offset line but at $Re_{nom} = 25 \times 10^6$, the disparities have virtually disappeared.

This result is taken as support for the contention that the flow visualization material used did not materially affect the boundary-layer development and that the reason for the lack of uniformity in drag (in the spanwise sense), at Re_{nom} = 12 and 17×10^6, largely lies in the widely varying lengths of laminar boundary layer that occur. The underlying reason for the varying length of laminar layer is still unknown but possibly stems from non-uniformity in upstream turbulence or leading-edge roughening due to the impact of microscopic particulate matter borne by the stream.

Some comparisons with calculated[11] shear stress coefficients are given in Fig.24 for $Re_{nom} = 12 \times 10^6$. At C_n = 0.25 the measured shear stress coefficient indicates a low value at x/c = 0.1 followed by a rapid increase to a 50% higher value at x/c = 0.15. These results indicate a short bubble separation. On the assumption of transition at x/c = 0.05, the calculated boundary-layer yields a value of Reynolds number, based on local conditions for velocity, density and viscosity and using the displacement thickness as reference length, of about 2000 at x/c = 0.05. This is substantially greater than Crabtree's criterion[12] for the formation of a short bubble and suggests that separation took place some short distance ahead of x/c = 0.05. At the two higher values of Re_{nom} the low shear stress near the leading edge was not observed.

4. CONCLUSIONS

The aerofoil section NACA 65_1-213 (a=0.5) has been subjected to measurements of surface pressure distribution, overall forces, wake pressures and skin friction for Mach numbers and loading producing shock waves at chord Reynolds numbers overlapping flight values. Through a comprehensive set of measurements of surface pressure on two chordwise lines and surface flow direction flow visualization it has been established that this particular model suffers from a significantly curved shock wave (in plan view) for high enough values of Mach number and normal force coefficient. It is difficult to assign strict limits, since matters are complicated by there being a Reynolds number dependence, but as an example we can claim that at a Mach number of 0.76 there would be small curvature up to C_n = 0.3 for Reynolds number between 25 and 44×10^6 and a suction velocity ratio $V_n/U_\infty = 0.0054$. At Re = 53×10^6 it appears that an increased amount of suction is required.

For a Mach number of 0.8 a reduction in V_n/U_∞ appears warranted at least in the range 35 - 53×10^6 and that with the proper value, satisfactorily straight shocks might be obtained up to C_n = 0.3.

The availability of full-scale flight measurements has been valuable in arriving at an assessment of the validity of some of the pressure distributions measured in the wind tunnel. They support the present method of applying sidewall boundary-layer control.

As reported in other establishments confidence in the results of wake drag measurements suffers from the realization of poor uniformity in the spanwise direction. In the NAE high Reynolds number facility it has been found that the gross discrepancies noted at 12 and 17×10^6 are, at least in part, at a nominal Mach No. of 0.7, because of an uneven distribution of skin friction in the spanwise sense.

The effect of Reynolds number on upper surface shock wave position for the NACA 65_1-213 (a=0.5) aerofoil for $12 \times 10^6 \leq Re \leq 55 \times 10^6$ has been investigated. Having in mind the limitations imposed by the curved shock-wave phenomenon, we, nevertheless, think that for moderate C_n (up to 0.3) upper-surface shock-wave position is still somewhat affected by Reynolds number increases above about 50×10^6. Below M_T = 0.76 the shock wave location shift is very small for Reynolds numbers between 12 and 53×10^6 (about 1% chord for C_n = 0.1) but above that Mach number the movement is nearly 6%. While significant, the latter figure is about one-third of the shifts that have been observed between results obtained at the usual chord Reynolds number of complete model testing in wind tunnels and full-scale flight[9].

In addition to their value in demonstrating the spanwise variation in surface shear stress, with its Reynolds number dependence, it is felt that the razor blade measurements have underlined the utility of this method of measuring skin friction on an aerofoil. The bonding of the blades to the surface with a very thin cement proved to be acceptable even in the rather harsh starting environment of a blowdown wind tunnel.

The measured values of shear stress coefficient are in fair accord with calculated quantities and demonstrate the utility of the calibration equation of reference 10 with respect to friction measurements in the presence of unfavourable pressure gradients.

It may be noted that the test procedure involved one tunnel run for each pair of C_f values (upper and lower surface). This devolved from a decision to investigate the effect, if any, of upstream blades, on the pressures sensed by those downstream. For the sake of economical testing it was hoped to find only a small interference, since the blade spacings were 375 blade thicknesses (1.5"). This however proved not to be the case and changes of up to 5% in the apparent value of C_f appeared when the C_f profile was computed from measurements taken with all blades in place. For a chord Reynolds number of 25×10^6 or greater however, it would still be possible to obtain a profile with only two runs (one run to establish the basic pressure distribution) by employing a model with two or more staggered rows of pressure holes.

The results for normal force, drag and pitching moment are presented in terms of results which are uncorrected for the effect of the perforated upper and lower walls of the test section. For the Mach number range used, the corrections[13] to angle of incidence give, approximately

$$\alpha^\circ = \alpha_g^\circ - 2.4\, C_n$$

The corrections to lift coefficient and pitching moment are negligibly small and the correction to Mach number for solid and wake blockage reduces the test Mach number by 0.005, at most.

SYMBOLS

U	Stream velocity
M	Mach number
Re	Reynolds number based on aerofoil chord
α_g	angle between aerofoil chord line and wind tunnel centre line
α	angle of attack
c	aerofoil chord
b	duct width (15 inches)
h	duct height (60 inches)
v_n	averaged velocity through suction plates in sidewalls

Oxyz	coordinate system, origin at intersection of sidewall balance centre line and working section centre line. x measured +ve downstream, y measured +ve to right, z measured +ve upward
S	distance along aerofoil surface from leading edge
Y_ℓ	distance from centre line of aerofoil to offset line of pressure taps
x_s	position of normal shock on aerofoil, relative to leading-edge
Δx_s	difference between position of normal shock on aerofoil centre-line and on offset line of pressure taps
C_p	pressure coefficient
C_n	normal force coefficient
C_c	chordwise force coefficient
ΔC_n	$C_{np} - C_{nb}$
Δ	constant in the razor blade calibration equation(10)
$C_{mc/4}$	quarter chord pitching moment coefficient
C_d	drag coefficient
C_f	shear stress coefficient

Subscripts

nom	nominal
T	test value
∞	free stream value
p	pressure derived
b	balance derived
w	wake
m	measured
d	design

Superscripts

*	critical value

REFERENCES

1. Ohman,L.H. (Ed): The NAE High Reynolds number 15 in.x60 in. two-dimensional test facility. Part I, General Information. Ohman,L.H. and Brown,D: Part II Results of initial calibration. NAE LTR-HA-4.

2. Ohman,L.H.,Brown,D.: The NAE High Reynolds number 15 in. x 60 in. two-dimensional test facility, description, operating experiences and some representative results. AIAA No.71-293 (AIAA 6th Aerodynamic Testing Conference 1971).

3. Ohman,L.H.,Kacprzynski,J.,Brown,D.: Some results from tests in the NAE High Reynolds number two-dimensional test facility on "shockless" and other aerofoils. ICAS Ppaer 72-33. The 8th Congress of the International Council of the Aeronautical Sciences.

4. Brown,H.H. and Clousing,L.A.: Wing pressure measurements up to 0.866 Mach number in flight on a jet propelled airplane. NACA Technical Note 1181 (1947).

5. Thompson,B.G.,Carr-Hill, G.A.,Powell,B.J.: A programme of research into viscous aspects of flow on swept wings. NPL Aero Note 1100 1970.

6. Pearcey,H.H.,Holder,D.W.: Examples of the effects of shock, induced boundary layer separation in transonic flight. ARC R & M 3510, 1967.

7. Gadd,G.E.: Interactions between normal shock waves and turbulent boundary layers. ARC R & M 3262, 1962.

8. Loving,D.L.: Wind tunnel flight correlation of shock induced separated flow. NASA TND 3580, 1966.

9. Blackwell,J.A. Jr. Effect of Reynolds number and boundary layer transition location on shock induced separation. Transonic Aerodynamics, AGARD Specialists Meeting, Paris, Sept.1968.

10. Cook,T.A.: Measurements of the boundary-layer and wake of two aerofoil sections at high Reynolds numbers and high subsonic Mach numbers. RAE TR 71127(1971)

11. Nash,J.F.,Macdonald,A.G.: The calculation of momentum thickness in a turbulent boundary layer at Mach numbers up to unity. ARC CP No.963 (1967).

12. Crabtree,L.F.: The formation of regions of separated flow on wing surfaces. ARC R & M 3122, 1957.

13. Mokry,M.: Higher order theory of two-dimensional subsonic wall interference in a perforated wall wind tunnel. NRC NAE LR-553.

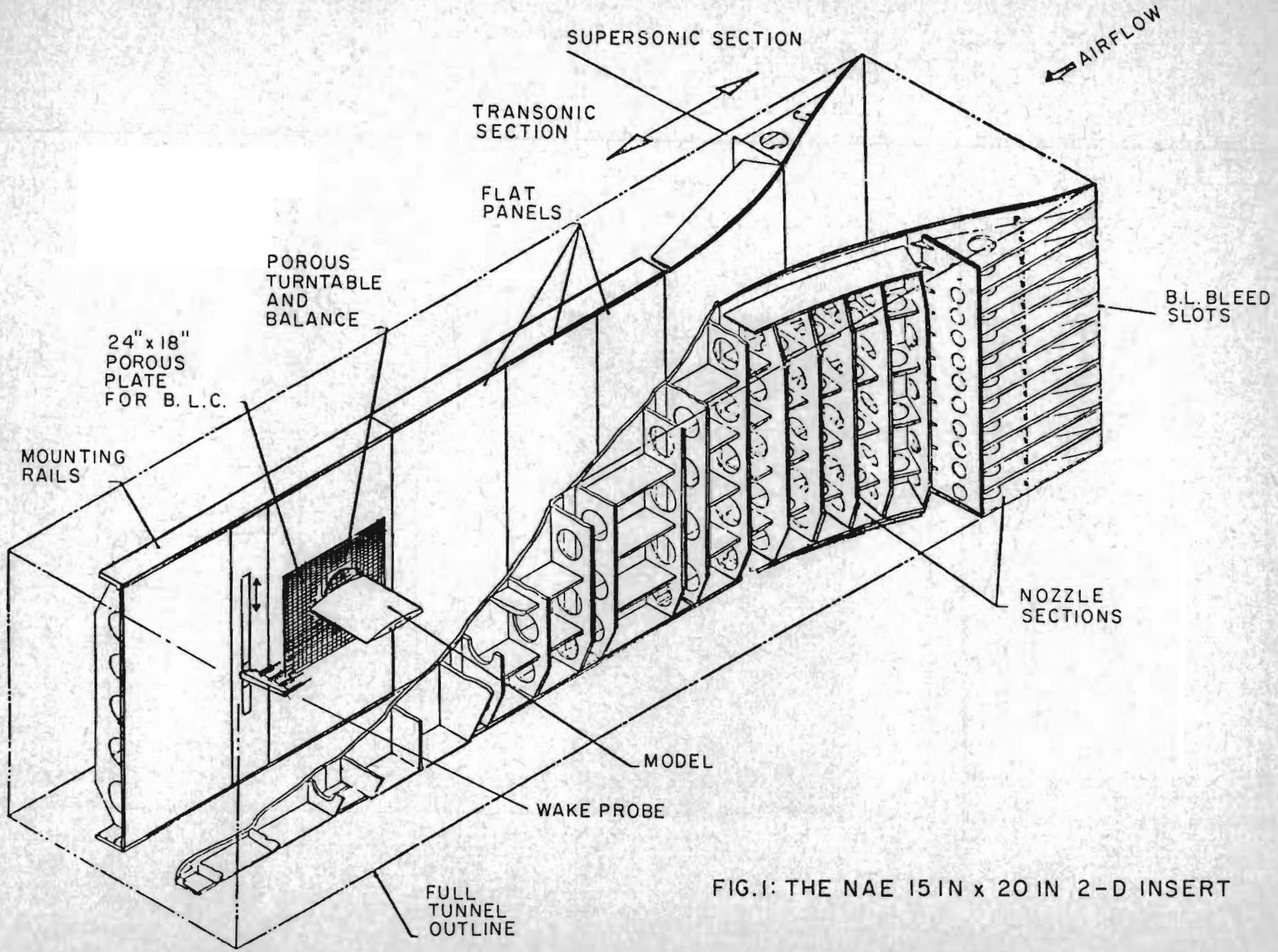

FIG. 1: THE NAE 15 IN x 20 IN 2-D INSERT

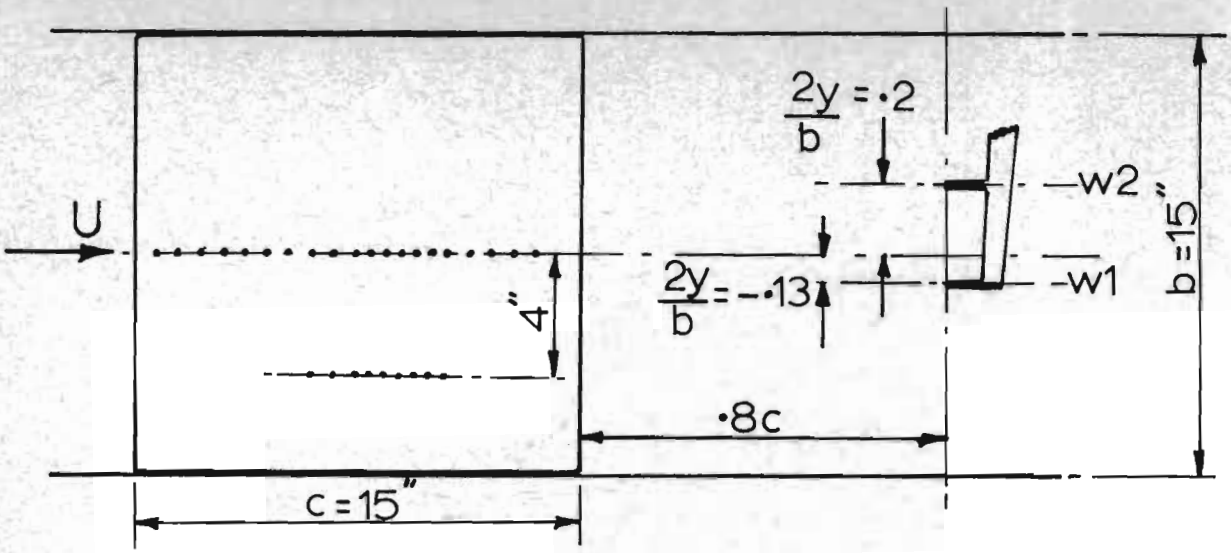

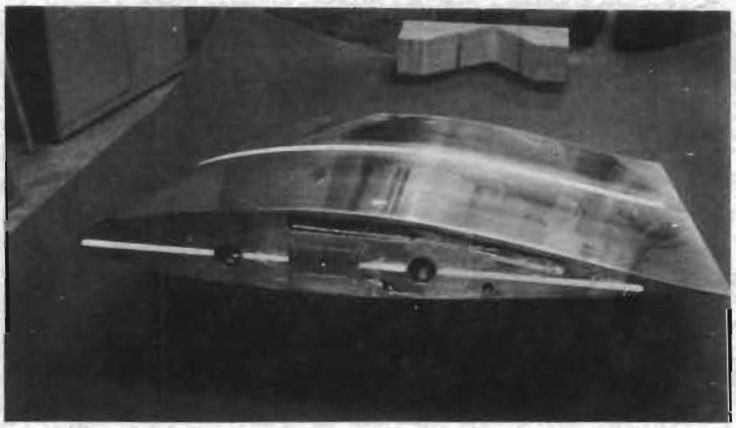

(a)

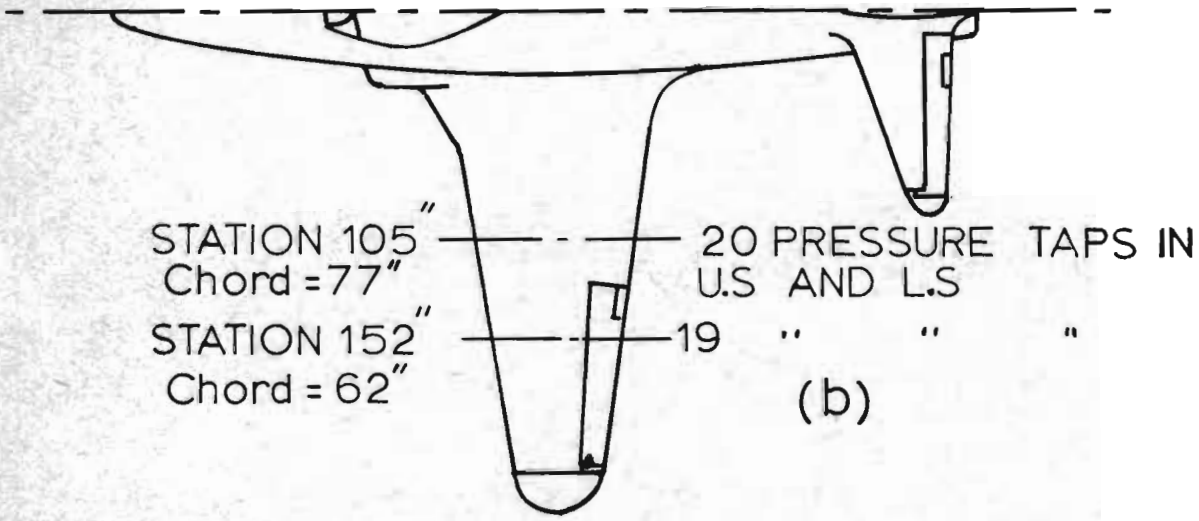

(b)

FIG.2 (a) AEROFOIL MODEL–NACA 65,-213(a=.5).
(b) FLIGHT TEST AIRCRAFT

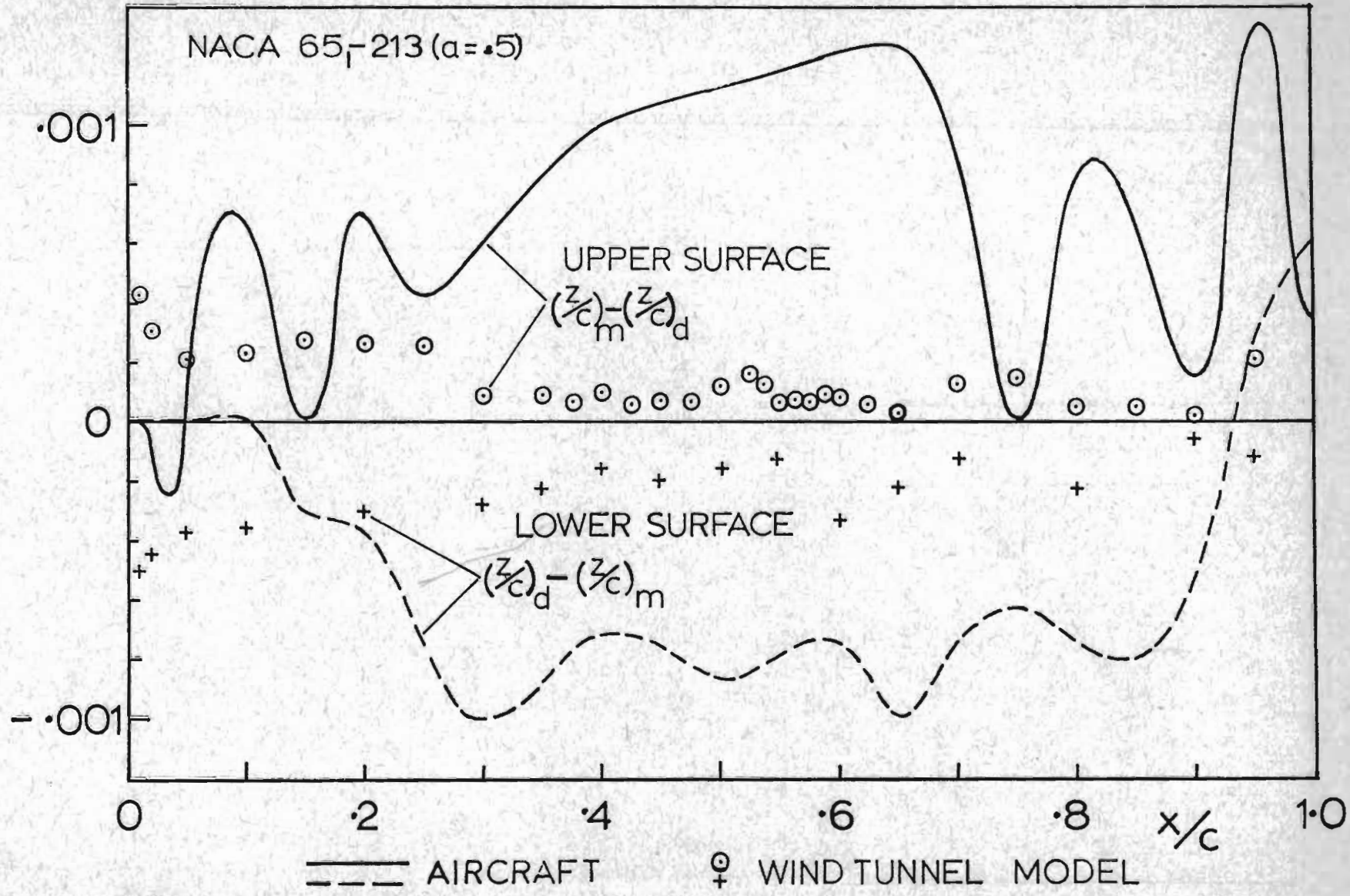

FIG.3 AEROFOIL SECTION PROFILE ACCURACY

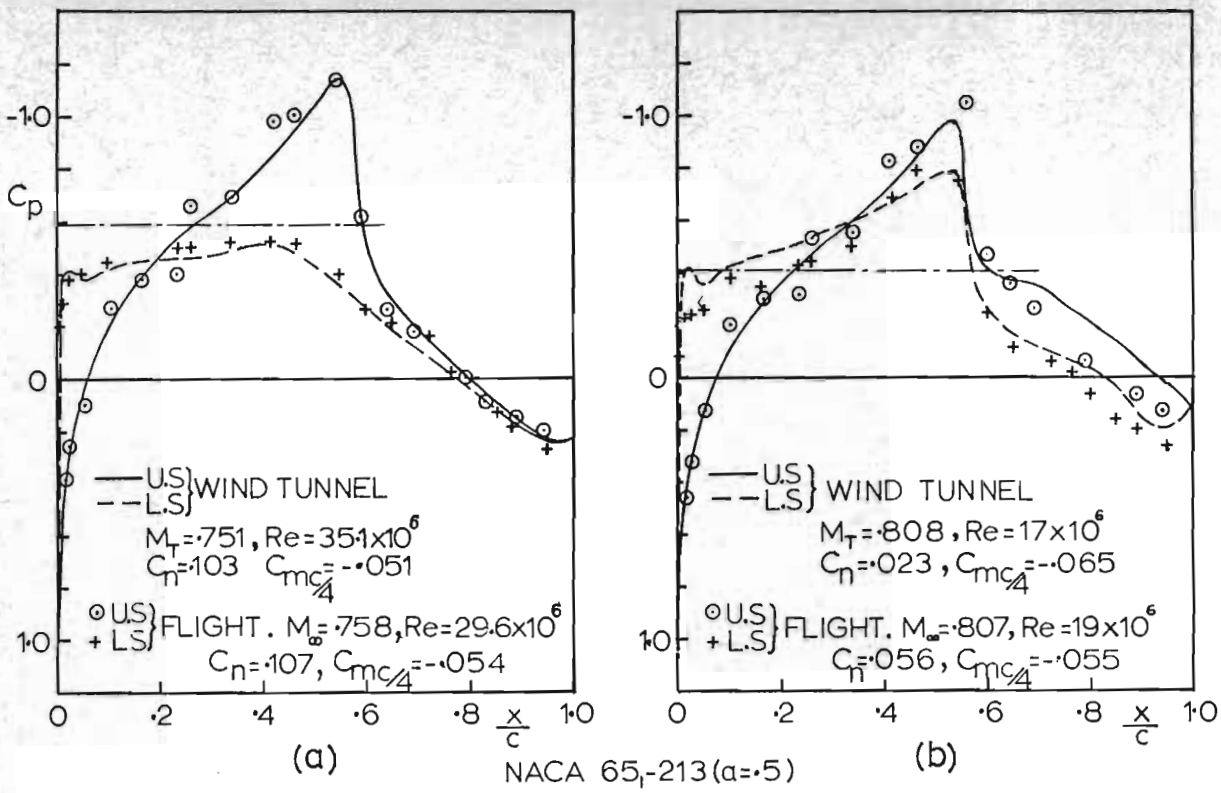

FIG.4 WIND-TUNNEL AND FLIGHT-TEST PRESSURE DISTRIBUTIONS.

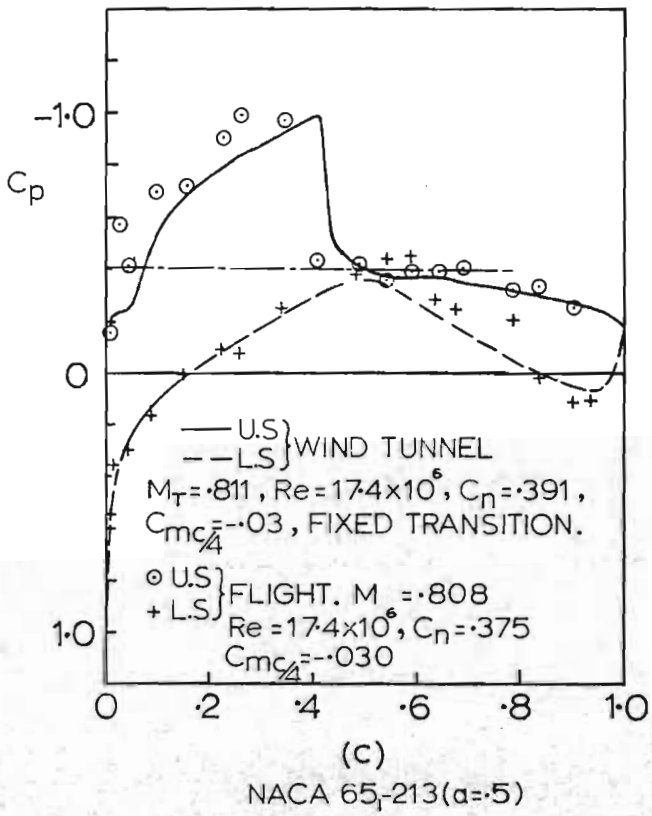

FIG.4 (CONCLUDED)

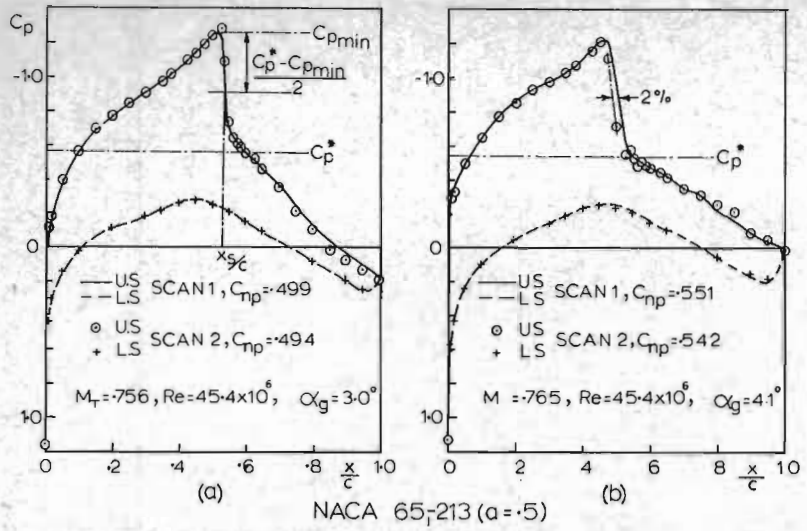

NACA 65$_1$-213 (a=·5)

FIG.5 UNSTEADINESS IN UPPER SURFACE SHOCK POSITION.

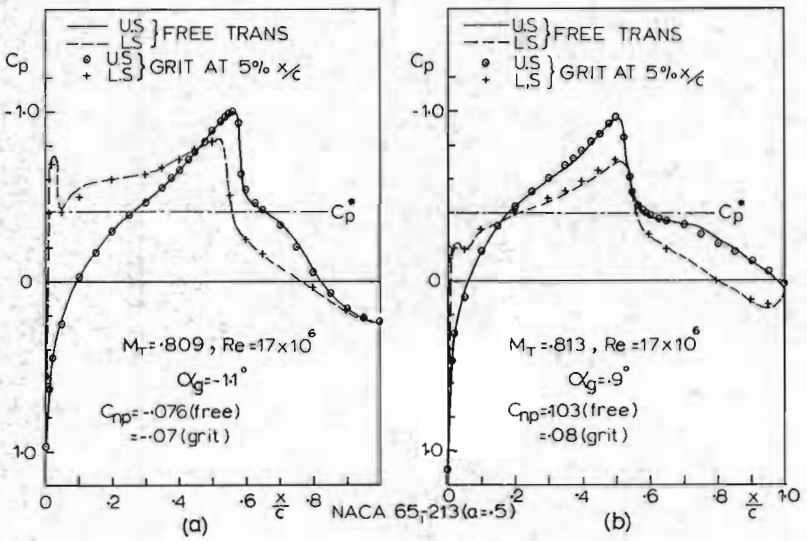

NACA 65$_1$-213(a=·5)

FIG.6 THE EFFECT OF A ROUGHNESS STRIP ON PRESSURE DISTRIBUTION.

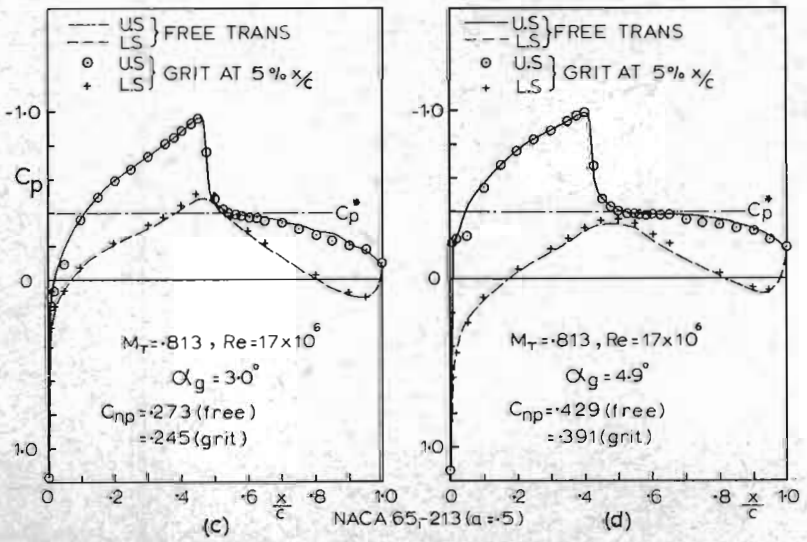

NACA 65$_1$-213 (a=·5)

FIG.6 (CONCLUDED)

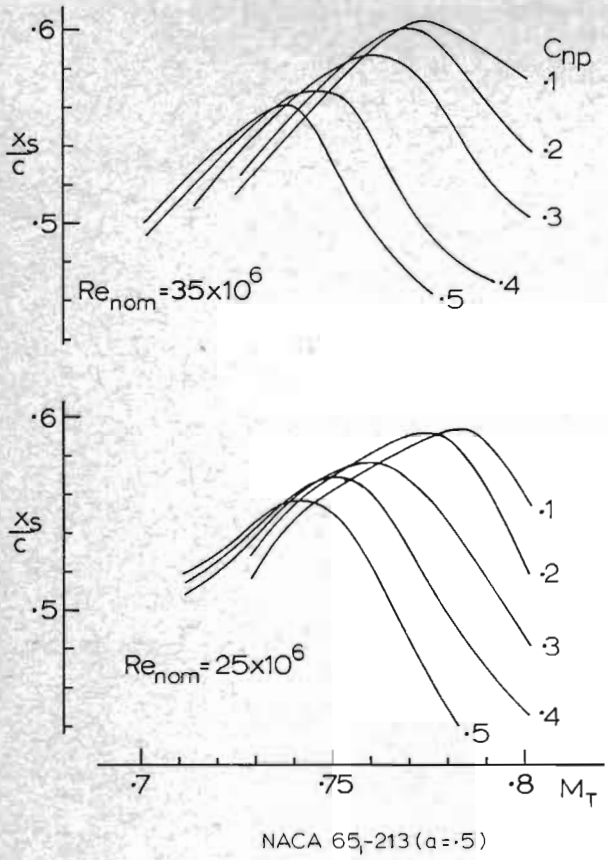

NACA 65$_1$-213 (a = ·5)

FIG.7 UPPER-SURFACE SHOCK POSITION VERSUS MACH NUMBER AND NORMAL-FORCE COEFFICIENT.

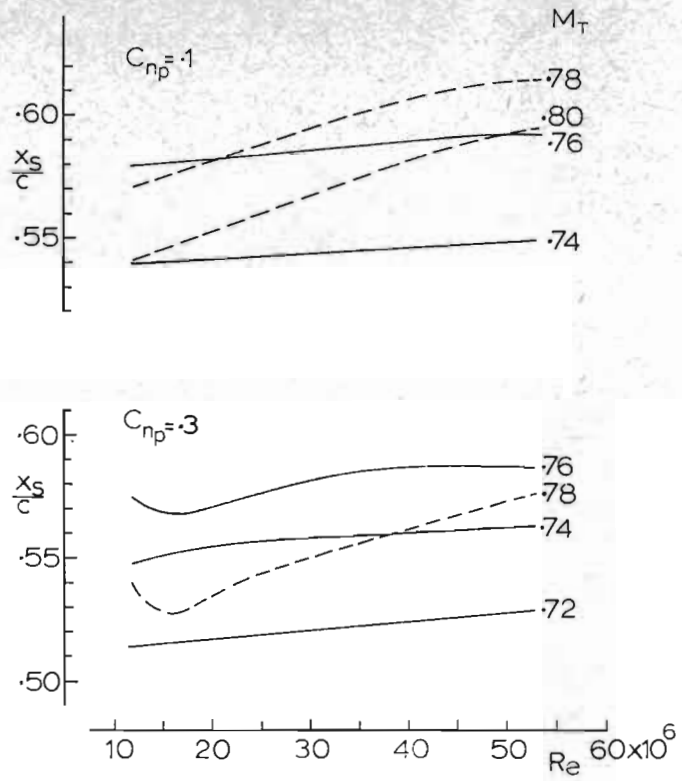

NACA 65$_1$ 213 a = ·5

FIG.8 INFLUENCE OF REYNOLDS NUMBER ON UPPER SURFACE SHOCK POSITION.

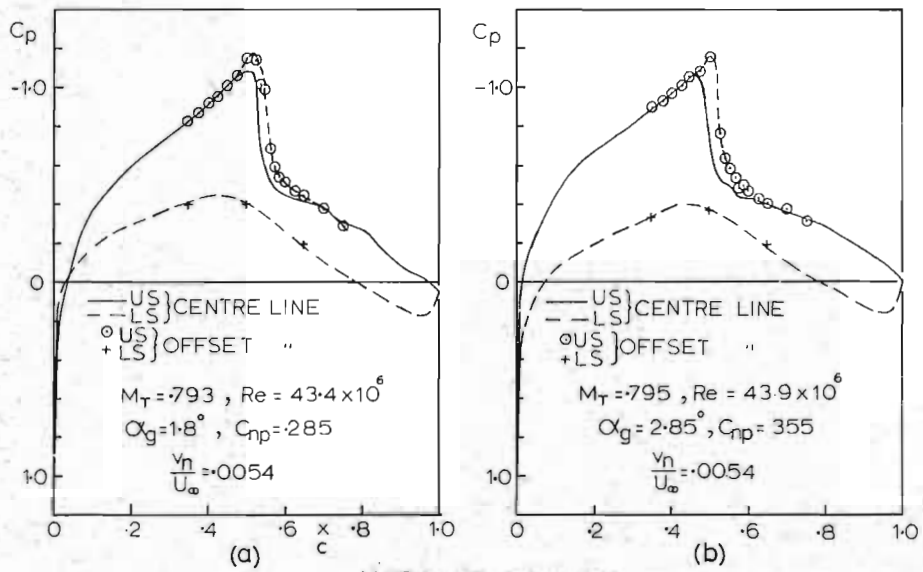

NACA 65$_1$ 213 a = ·5

FIG.9 SHOCK CURVATURE EFFECT ON PRESSURE DISTRIBUTION.

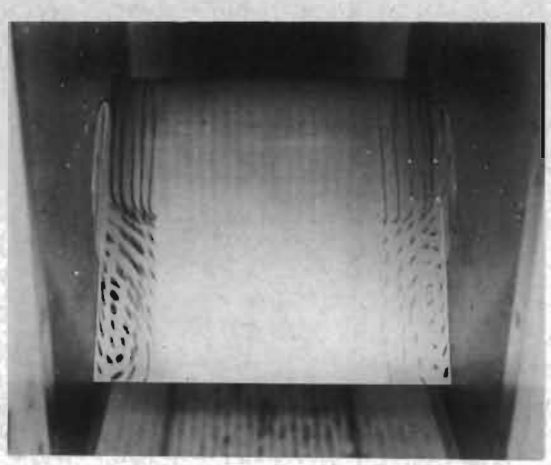

$M_{nom} = .75$, $Re_{nom} = 12 \times 10^6$
$\alpha_g = 5°$, $(v_n/U_\infty = .0045)$

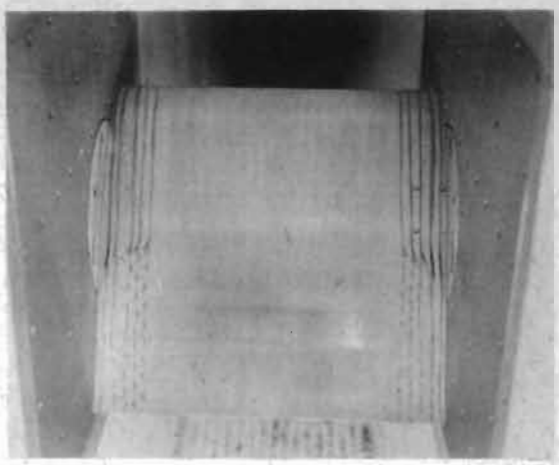

$M_{nom} = .75$, $Re_{nom} = 25 \times 10^6$
$\alpha_g = 5°$

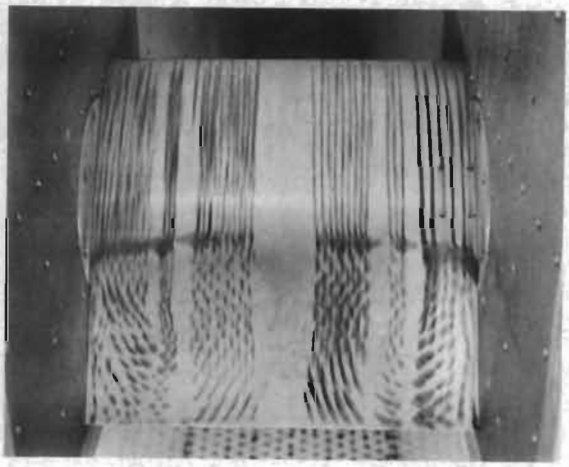

$M_{nom} = .8$, $Re_{nom} = 25 \times 10^6$
$\alpha_g = 3°$

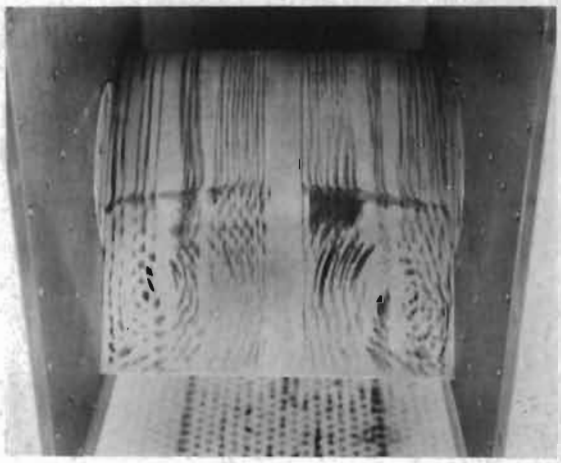

$M_{nom} = .8$, $Re_{nom} = 25 \times 10^6$
$\alpha_g = 5°$

FIG.10 OIL STREAK RECORDS OF UPPER SURFACE SHOCK WAVE CURVATURE. (NACA 65_1-213 (a=.5) SECTION)
$v_n/U_\infty = .0054$

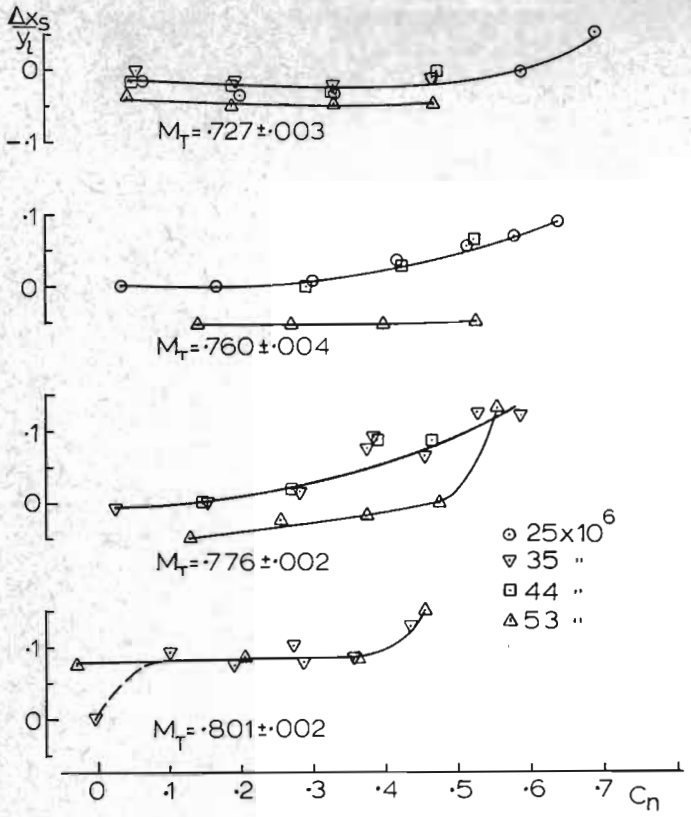

FIG.11 UPPER-SURFACE SHOCK CURVATURE ON NACA 65$_1$-213(a=·5) PROFILE (v_n/U_∞=·0054)

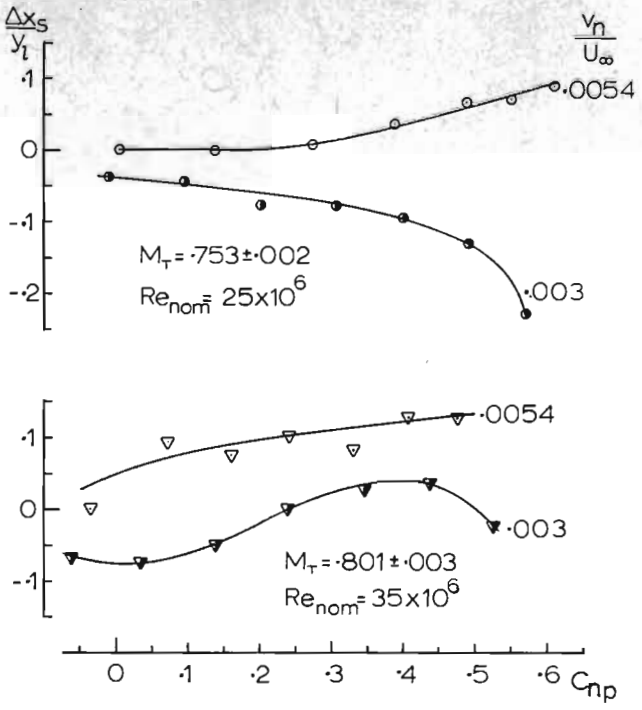

FIG.12 THE EFFECT OF WALL BOUNDARY-LAYER REMOVAL ON UPPER SURFACE SHOCK-WAVE CURVATURE.

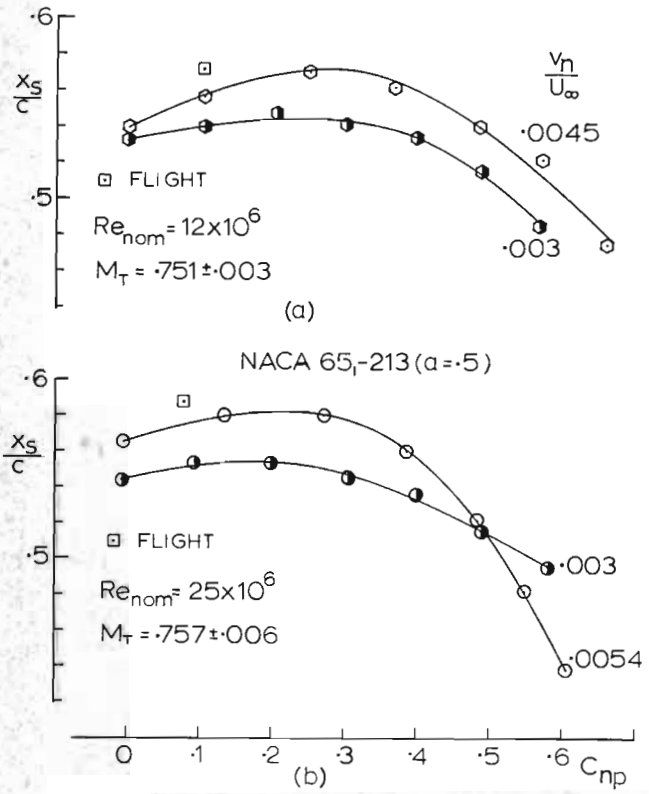

FIG.13 THE EFFECT OF WALL BOUNDARY LAYER REMOVAL ON UPPER-SURFACE SHOCK-WAVE POSITION.

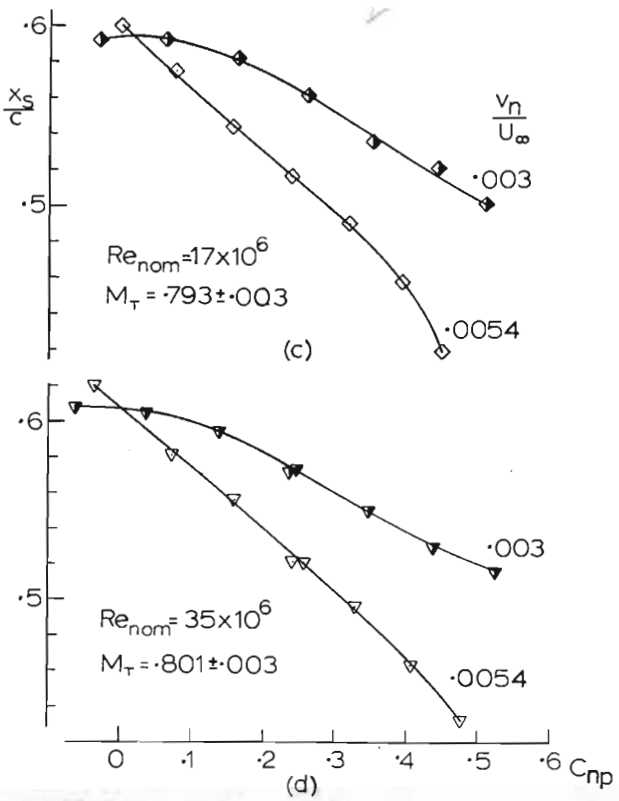

FIG.13 (Concluded)

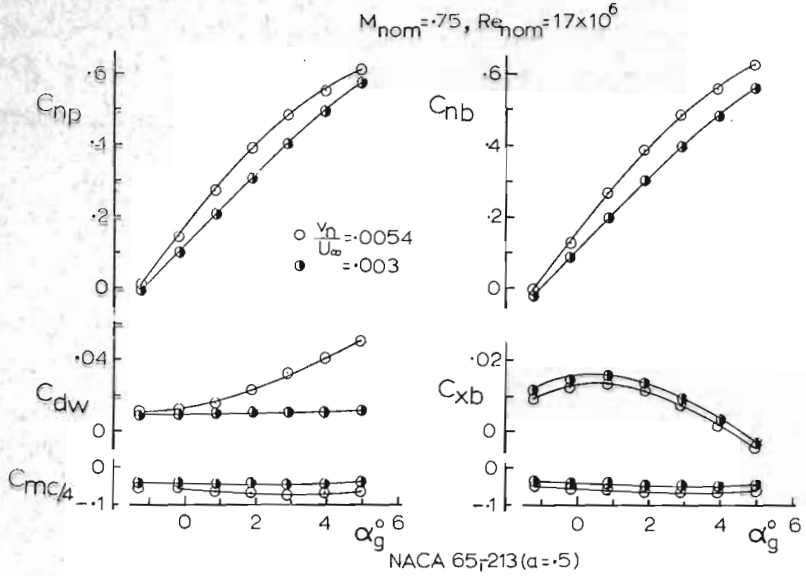

FIG14(a) THE EFFECT OF WALL BOUNDARY-LAYER REMOVAL ON MEASURED FORCE COEFFICIENTS

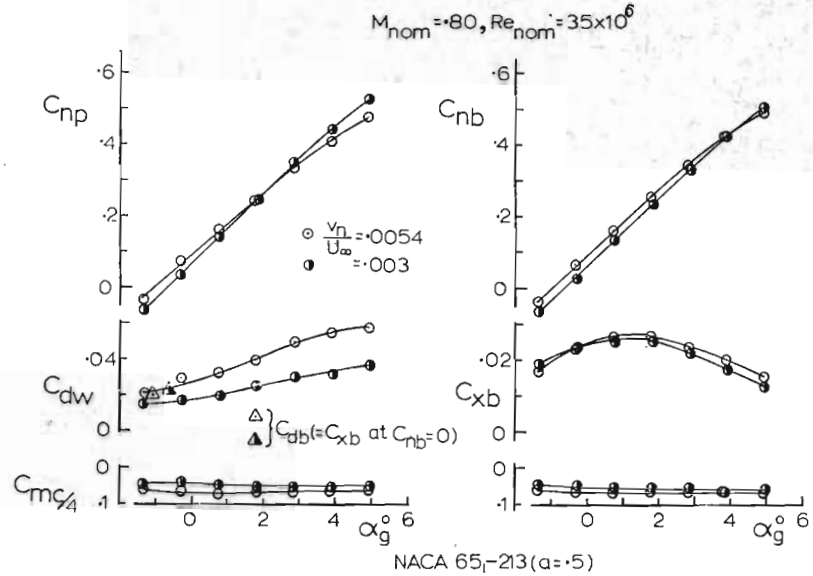

FIG14(b) THE EFFECT OF WALL BOUNDARY-LAYER REMOVAL ON MEASURED FORCE COEFFICIENTS

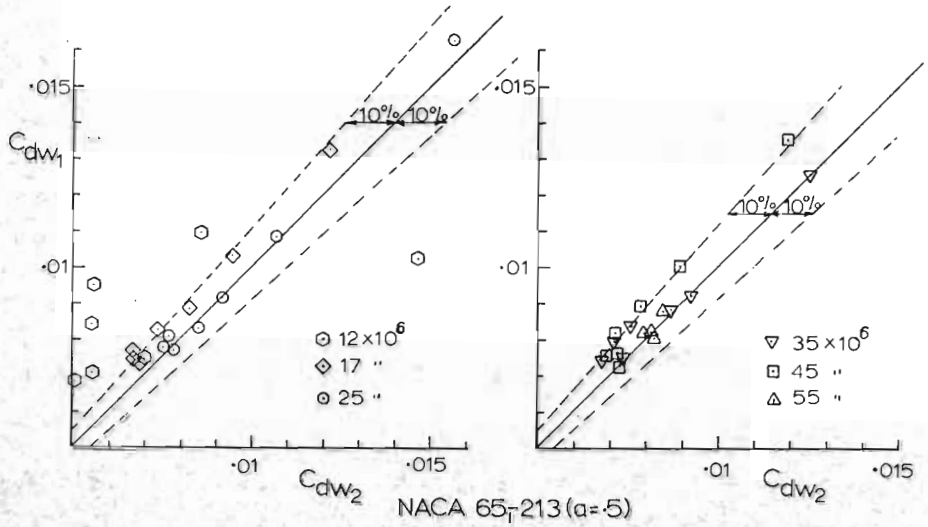

FIG.15 EFFECT OF REYNOLDS NUMBER ON WAKE-DRAG UNIFORMITY (M_{nom}= ·7 , v_n/U_∞=·0054).

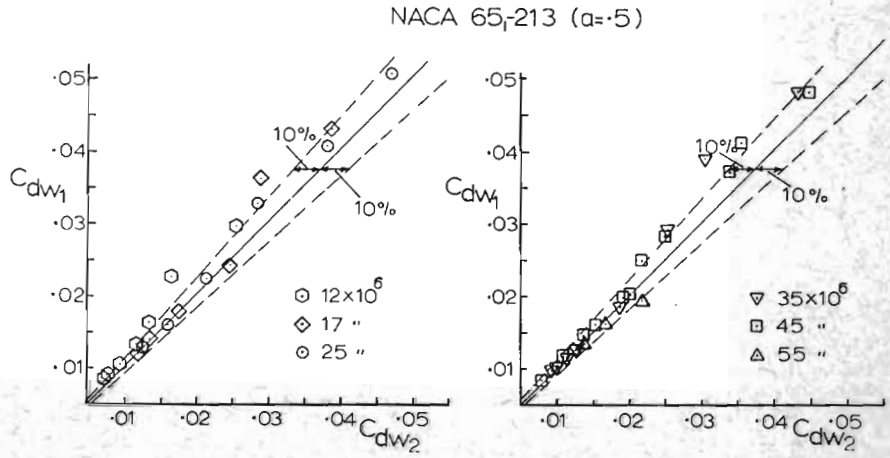

FIG.16 EFFECT OF REYNOLDS NUMBER ON WAKE-DRAG UNIFORMITY (M_{nom}=·75 , v_n/U_∞=·0054).

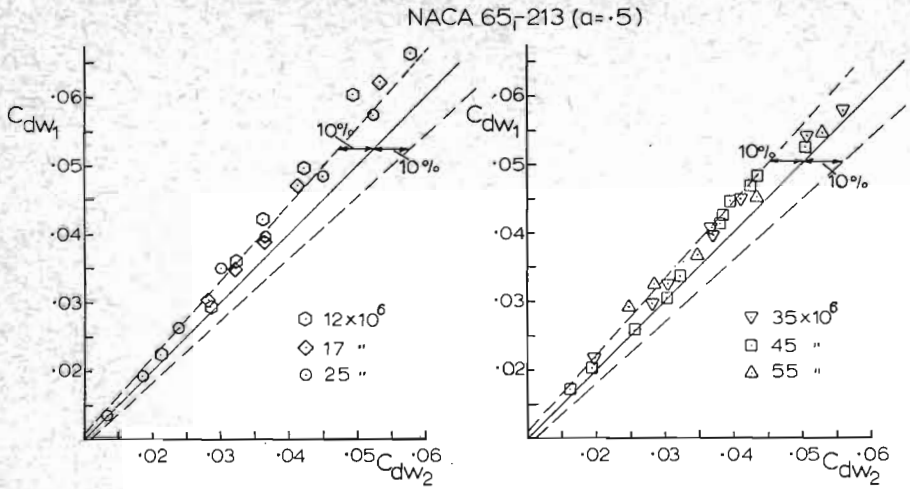

FIG.17 EFFECT OF REYNOLDS NUMBER ON WAKE-DRAG UNIFORMITY (M_{nom}=·80, v_n/U_∞=·0054).

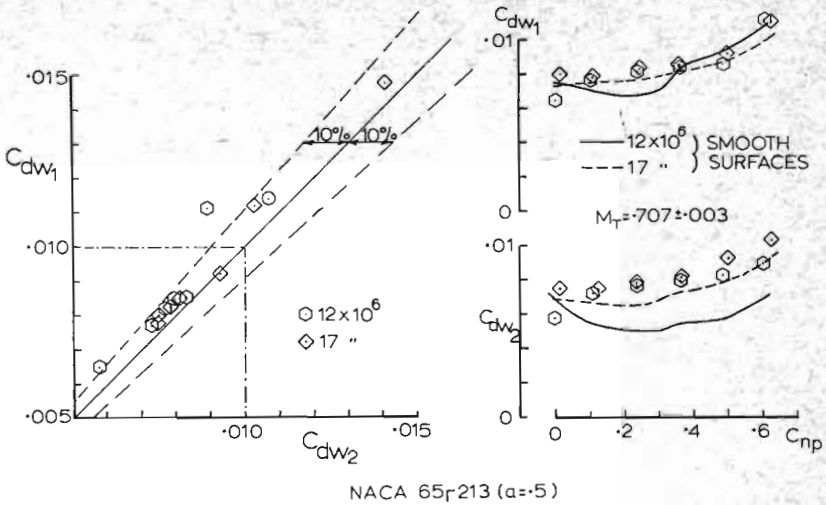

NACA 65$_1$213 (a=·5)

FIG.18 THE EFFECT OF A BOUNDARY-LAYER TRIP AT x/c= 5% ON WAKE-DRAG UNIFORMITY AND LEVEL (M_{nom}=·7).

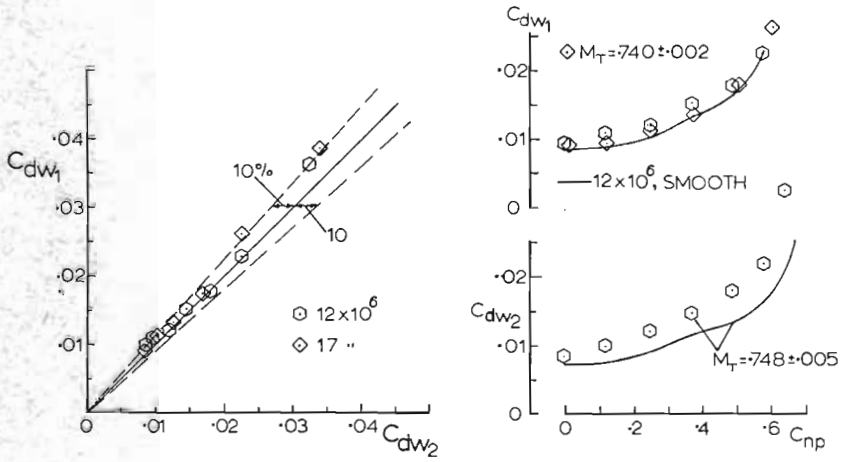

NACA 65$_1$-213 (a=·5)

FIG.19 THE EFFECT OF A BOUNDARY-LAYER TRIP AT x/c= 5% ON WAKE-DRAG UNIFORMITY AND LEVEL (M_{nom}=·75).

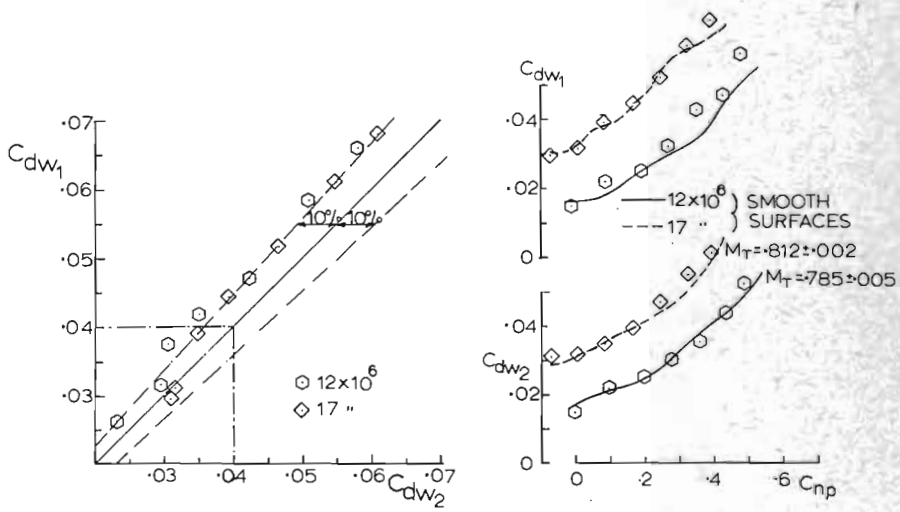

NACA 65$_1$-213 (a=·5)

FIG.20 THE EFFECT OF A BOUNDARY LAYER TRIP AT x/c= 5% ON WAKE DRAG UNIFORMITY AND LEVEL (M_{nom}=·8).

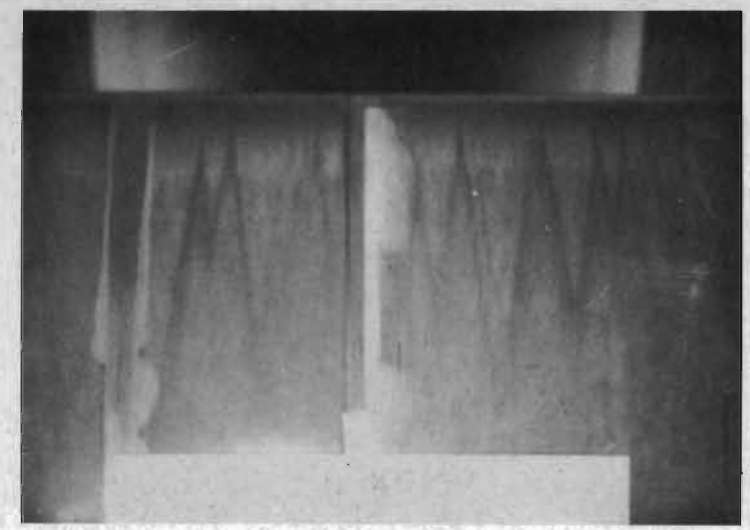

$Re_{nom} = 12 \times 10^6$

$\alpha_g = 0°$

$C_{np} = .12$

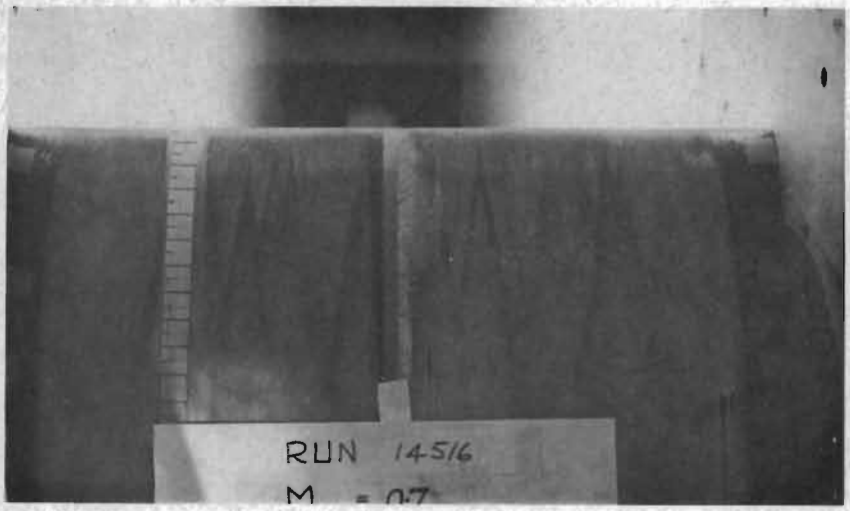

$Re_{nom} = 12 \times 10^6$

$\alpha_g = 2°$

$C_{np} = .34$

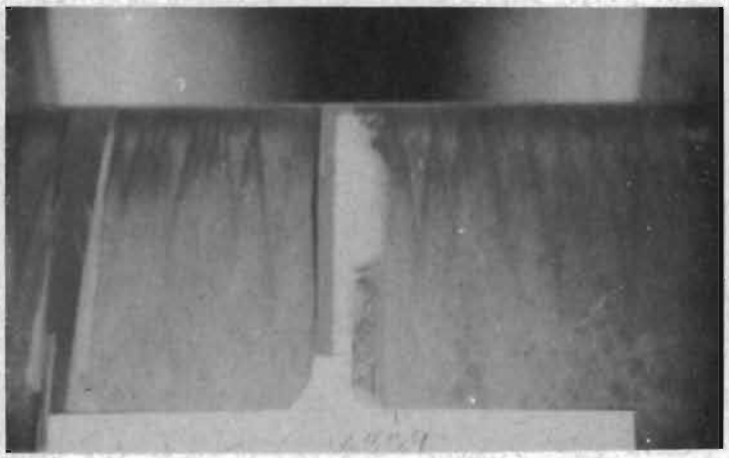

$Re_{nom} = 17 \times 10^6$

$\alpha_g = 0°$

$C_{np} = .12$

FIG.21 SURFACE FLOW VISUALIZATION, $M_{nom} = .7$. FREE TRANSITION.

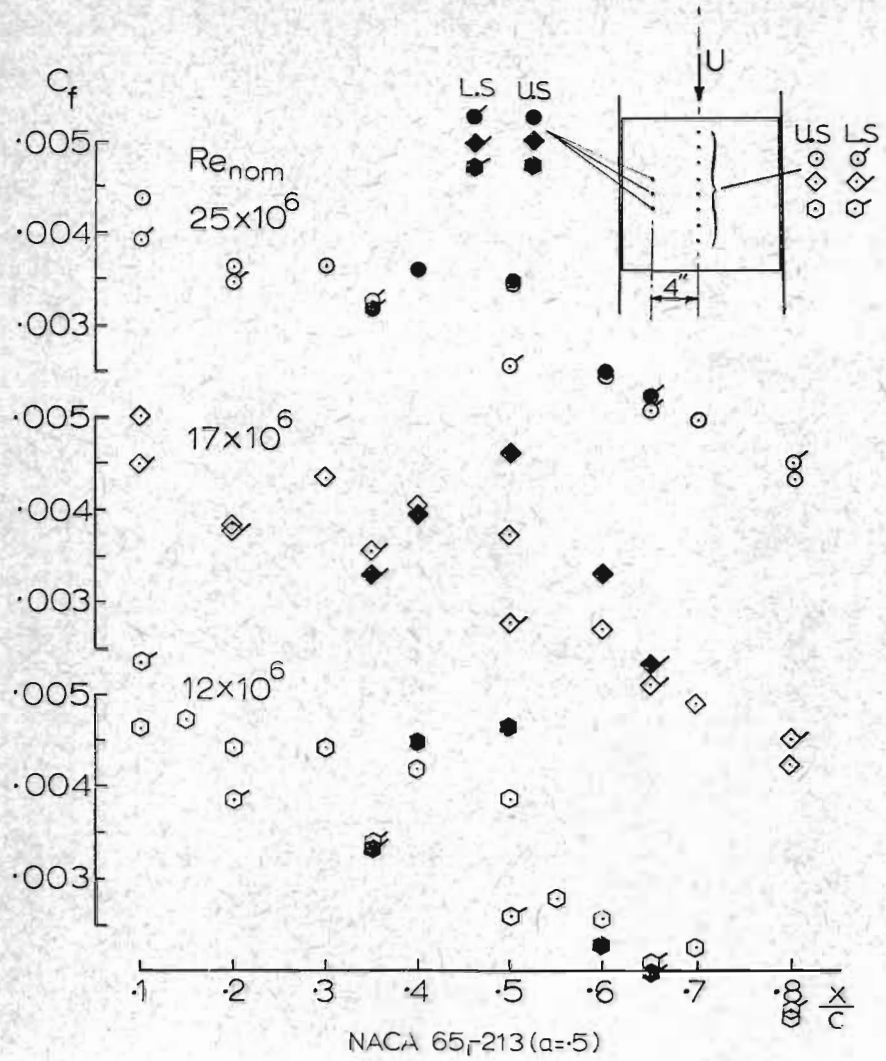

FIG.22 SPANWISE UNIFORMITY OF MEASURED SHEAR STRESS COEFFICIENT.
(M_{nom}=·7 , C_{nb}≏0)

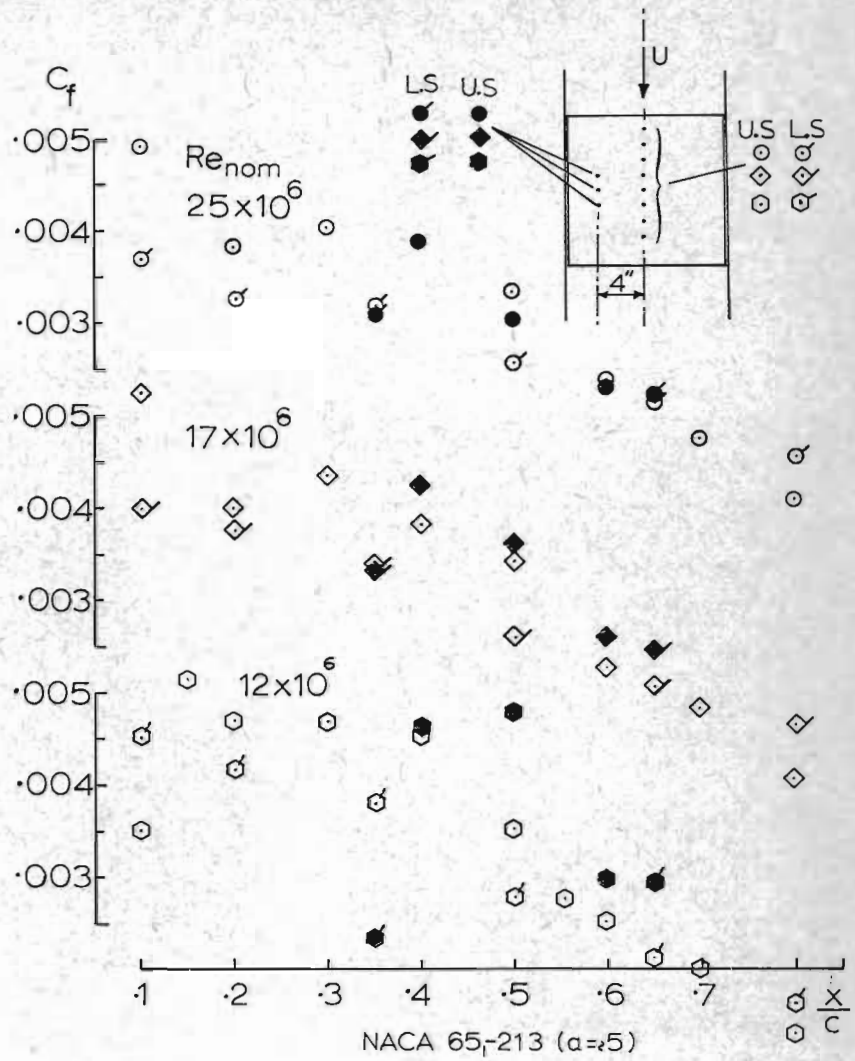

FIG.23 SPANWISE UNIFORMITY OF MEASURED SHEAR STRESS COEFFICIENT.
(M_{nom}=·7 , C_{nb}≏·25)

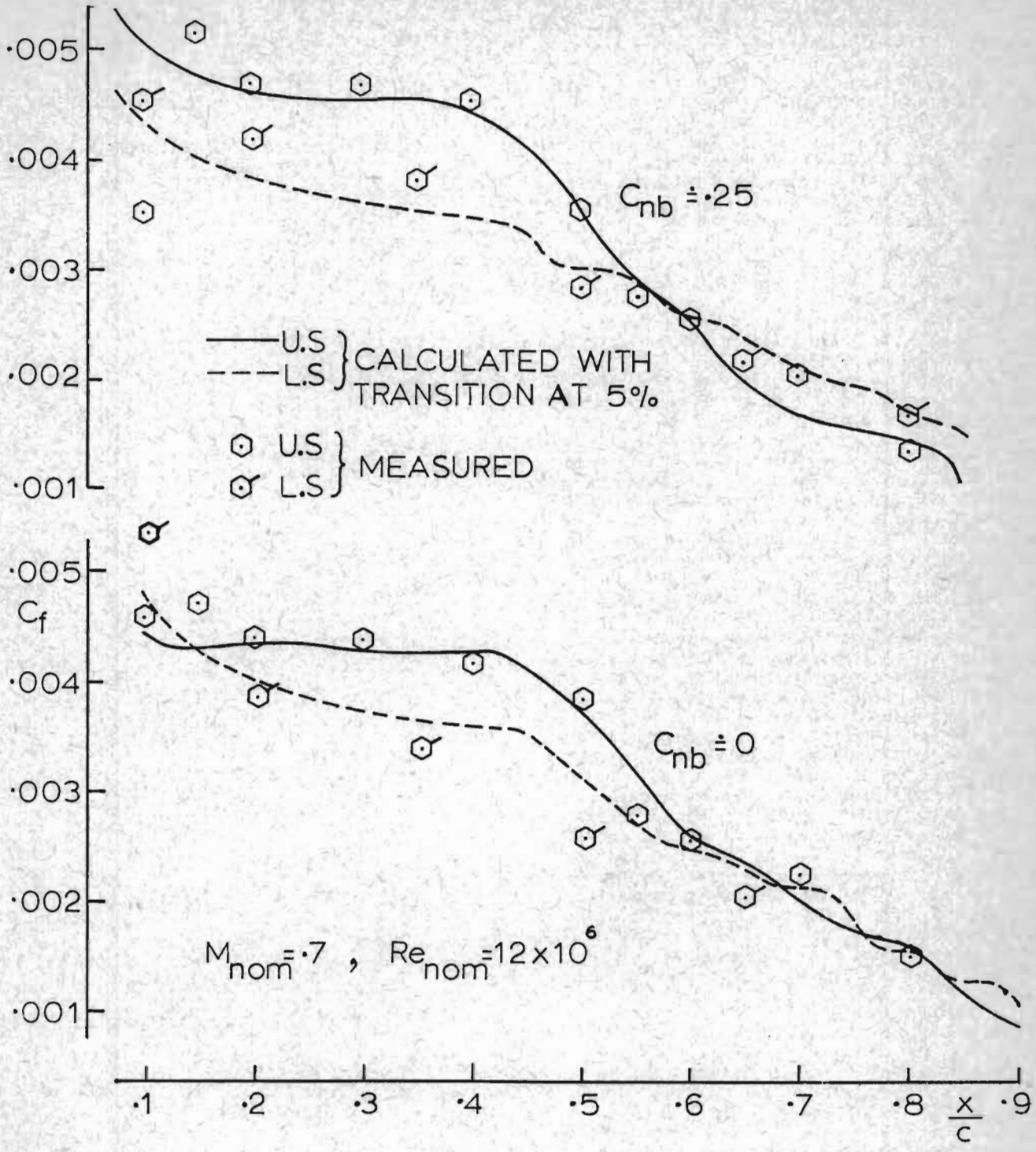

FIG.24 CALCULATED AND MEASURED SHEAR STRESS COEFFICIENTS.

DISCUSSION

G.M. Lilley (University of Southampton, U.K.): The changing results as the Mach number is increased and in particular the generation of curved shock waves leads one to seek explanation on the effect of the side wall boundary layers. Although the aerofoils are surrounded by a porous surface on the side wall is there evidence to indicate these panels are large enough to eliminate side wall boundary layer effects at the highest Mach number in these tests. Is it possible that the size of porous panel adequate for low Mach nominal 2-D tests will prove to be too small as Mach number is increased?

D. Brown: We have no direct evidence to either support or contradict the correctness of sizing of the porous panels through which the sidewall boundary layers are removed but, prior to the measurements on the model of NACA 65_1-213 section, the pehnomenon of the curved shock had not been seen.

It is conceivable that, given the right combination of free-stream Mach number and angle of incidence the upper surface (or lower) shock-wave would extend beyond the bounds of the perforated area. If the shock-wave were strong enough there would be separation of the sidewall boundary-layer on the unperforated walls but attached flow could still hold over the porous region. This could lead to a redistribution of the swallowing capacity of the working section downstream such as to cause a curved shock wave.

However the above remarks do not suggest any possibility that the shock could be curved forwards as well as backwards but we have consistent data (Fig. 11) showing that at intermediate Mach numbers the shock waves are curved forward at the highest Reynolds number. At this time we have not made any investigations into the cause of this complication.

It is worth noting that on the porous plates the boundary layer is expected to decrease in thickness in the downstream direction. Beyond the sonic line there would be a flow acceleration due to the increase in effective duct width. If the majority of this effect were confined to a region near the walls, so that at a given station the velocity increases towards them, then the terminal shock wave would be backwards curved. The inference to be drawn from this argument is that at some Reynolds number between 44 and 53×10^6 the distribution of velocity normal to the porous surface altered so that the boundary layer is no longer decreased in the above manner.

B.G. Newman (McGill University, Canada): How did you correct the pressure measurements on the Lockheed aircraft for finite-wing effects?

D. Brown: The wing surface pressure distributions obtained from flight were not corrected for finite wing effects. It was assumed that the wing sections for which measurements are shown are sufficiently remote from wing tip and fuselage for any corrections to be negligible.

It can be shown that the effect of semi-infinite vortex lines emanating from the mid chord point at the 90% semi-span sections is, for the conditions noted in Fig. 4(a), such as to increase the pressure coefficient at the wing section for which measurements are shown by less than 0.01. The displacement effect of the fuselage decreases the pressure coefficient on the wing by approximately the same amount, according to the calculations of Labrujere et al (Paper 11, AGARD-CP-71-71).

There may be some high C_L cases where a correction would be necessary with this geometry but it is felt that in most cases it is reasonable to neglect the finite wing effects.